ION COLLECTION FROM A PLASMA BY A PINHOLE

David B. Snyder
NASA Lewis Research Center, Cleveland, OH

Joel L. Herr
Sverdrup Technology, Inc., Cleveland, OH

ABSTRACT

Ion focusing by a biased pinhole is studied numerically. Laplace's equation is solved in three dimensions for cylindrical symmetry on a constant grid to determine the potential field produced by a biased pinhole in a dielectric material. Focusing factors are studied for ions of uniform incident velocity with a three dimensional Maxwellian distribution superimposed. Ion currents to the pinhole are found by particle tracking.

The focusing factor of positive ions as a function of initial velocity, temperature, injection radius and hole size is reported. For a typical Space Station Freedom environment (i.e. oxygen ions having a 4.5 eV ram energy, 0.1 eV temperature and a -140 V biased pinhole), a focusing factor of 13.35 is found for a 1.5 mm radius pinhole.

INTRODUCTION

Present designs for Space Station Freedom SSF will result in structure potentials negative from the ambient plasma by about 150 V. This gives rise to concerns about sputtering by collection of ambient ions. On a broad scale this effect will be a contamination concern, but should not directly damage SSF structure. However SSF structure is covered by an insulating oxide layer. If holes develop in the insulation, ions will be focused into the hole and the local sputtering rate enhanced. At these pinhole sites sputtering will be aggravated. It is the enhanced collection of ions at these sites which this paper discusses.

Considerable effort has already gone into understanding how electrons are collected from plasma. Experimental measurements have been performed (ref. 1, 2), and computational models have been developed (ref. 3-5) to understand the 'snapover' effect, where electron collection to pinholes is significantly enhanced at potentials of a few hundred volts positive. However since ion collection does not exhibit this effect (due to the lower secondary electron yields) the simpler problem has not been investigated as intensively.

Recently, as part of the Space Station Electrical Grounding Tiger Team effort, Vaughn (ref. 6) has measured focus factors for ion collection, and Katz et al (ref. 7) have performed some initial calculations.

The model presented here does not solve Poisson's equation. Instead it solves Laplace's equation with computationally convenient boundary conditions. Thus it represents a simplification of the actual problem. While the results will not be exact, the model permits considerable qualitative examination of issues, and quantitative estimates of sputtering rates.

MODEL

The approach taken in this work is to solve Laplace's equation for a pinhole geometry, then track ion trajectories through the potential field. Electric fields are calculated from this potential field, and the equations of motion solved to find the trajectories of particles attracted toward the hole. The collection enhancement (focusing factor) can be found by finding the radius where particles no longer hit inside the hole. This approach does not include space charge effects. An approximation for the plasma sheath is included by adjusting the height of the calculation space.

Potential Fields

The potential fields were found by using the Point Gauss-Siedel method to solve the cylindrical difference formulation of Laplace's equation in a rectangular grid. The depth of the hole is not included in the model. Instead it is considered to be a uniformly biased conductor. While this may not be reasonable for modeling debris damage, it is reasonable for modeling the effect of insulation damage when the insulation thickness is small compared to the hole radius. The

insulation is treated as being at the plasma potential, 0 V. This results in a lower boundary having two potentials. Inside the hole radius the potential is at the bias potential. Outside, it is zero, referenced to the plasma potential. The upper boundary is set to the plasma potential, zero.

The potential contours in figure 1 show that the potential drops off very rapidly, and the potential contours that extend large distances are of low magnitude. The potential at about 1 radius from the center of the hole drops to 31 % of the applied voltage. The potential varies most rapidly at the edge of the hole. This is the region of strongest electric field. Near the hole edge, for a negative potential hole, the electric field flux lines go up from the surface and down to the hole surface. This shows up in the trajectories of particles which nearly miss the hole edge but are forced up and into the midregion of the hole.

In order to satisfy Dirichlet-Neumann conditions and completely specify the problem, the inner (r=0) and outer boundaries must also be specified. The inner boundary is a center of cylindrical symmetry, so the radial component of the electric field, E_r, must be zero. The electric field on the outer boundary also approaches zero as the radius approaches infinity. For these calculations E_r is also set to zero at this boundary. Unfortunately, the trajectory of particles near the boundary are very sensitive to the boundary's existence. Particles near the outer boundary tend to fall straight to the surface. However, when the boundary is moved away those particles may have a considerably different trajectory. For this work the boundary was set far enough away from the hole that the focusing factor did not change. The trajectory of particles not hitting the hole will be incorrect, but that aspect of the problem will be irrelevant to the results of this calculation.

Electric Field

The electric fields obtained from the potential grid will be integrated in the equations of motion to yield particle trajectories. Therefore the interpolated electric field within each grid region must be consistent with a relatively continuous potential field. Discontinuities in the potential field between grid regions can cause the integrated kinetic energy accumulated by the particle to disagree with that expected from the potential at a point and energy will not be conserved. This turns out to be especially important near the edge of the hole where the potential changes rapidly in one grid spacing and the electric field is both large and rapidly varying with position.

To satisfy this criterion, the electric field is evaluated in the center of the grid, and using additional interpolated potential points the gradient of the electric field components are evaluated as illustrated in figure 2. Interpolated potential points are evaluated to satisfy Laplace's difference equation. That is, they are the average of the four surrounding points. Potentials at the center of the grid regions, P(r,h) are obtained from the potential grid, P(j,i). The potential at the center of the grid edge, P(r,i) can then be interpolated from the two nearby grid centers and the two nearby grid corners.

The electric field components at the center of the grid can now be evaluated from the grid edge potentials and the gradients can be evaluated using the corner potentials. The electric field can then be interpolated anywhere in the grid region. The electric fields calculated in this way are pinned to reproduce the corner potentials as well as the center of the grid edge. The resulting potential field is continuous between grid regions through these points, and constrains the rest of the edges from being too discontinuous.

This method does not add new information to the known values at the grid points. Rather it uses the known values, and interpolates between them in a relatively continuous manner. The procedure could be reiterated to generate as continuous a potential field as required.

Particle Tracking

Particle Trajectories are found by integrating the equation of motion, $\mathbf{a} = \mathbf{F}/m$ to obtain velocity ($\mathbf{v}$) and position ($\mathbf{r}$). The electric field, $\mathbf{E}$, is evaluated either for calculation purposes relative to the center of the grid region, $\mathbf{r}_o$, or, for integration purposes relative to the position at the beginning of a time step, $\mathbf{r}(0)$,

$$\mathbf{E}(\mathbf{r}) = \mathbf{E}(\mathbf{r}(0)) + (\mathbf{r}-\mathbf{r}(0))\bullet\nabla\mathbf{E}.$$

The acceleration is given by,

$$\mathbf{a} = q/m\,[\mathbf{E}(\mathbf{r}(0)) + (\mathbf{r}-\mathbf{r}(0))\bullet\nabla\mathbf{E}]$$

the velocity is obtained from,

$$\mathbf{v}(T) = \mathbf{v}(0) + {}_0\!\int^{T} \mathbf{a}\, dt.$$

The first order expansion of $\mathbf{E}$ may be used to replace $\mathbf{a}$. An integrable estimate of r can be obtained by noting that,

$$\mathbf{r}(t) \sim \mathbf{r}(0) + \mathbf{v}(0)t + q/2m\ \mathbf{E}(\mathbf{r}(0))t^2,$$

as long as the term $(\mathbf{r}(t)-\mathbf{r}(0))\bullet\nabla\mathbf{E}$ is small compared to $\mathbf{E}(\mathbf{r}(0))$.
v can be iterated using,

$$\mathbf{v}(T) = \mathbf{v}(0) + q/m\ \mathbf{E}(\mathbf{r}(0))T$$

$$+ {}_0\!\int^{T} [\mathbf{v}(0)t + q/2m\ \mathbf{E}(\mathbf{r}(0))t^2]\bullet\nabla\mathbf{E}\, dt$$

finally,

$$\mathbf{v}(T) = \mathbf{v}(0) + q/m\ \mathbf{E}(\mathbf{r}(0))T + q/m\,[\mathbf{v}(0)T^2/2 + q/6m\ \mathbf{E}(\mathbf{r}(0))T^3]\bullet\nabla\mathbf{E}$$

similarly,

$$\mathbf{r}(T) = \mathbf{r}(0) + \mathbf{v}(0)T + q/2m\ \mathbf{E}(\mathbf{r}(0))T^2 + q/6m\ [\mathbf{v}(0)T^3 + q/4m\ \mathbf{E}(\mathbf{r}(0))T^4] \bullet \nabla \mathbf{E}$$

It is possible to take fairly large spatial steps using this formulation. The main constraint is to prevent the particle from moving too far into the next grid region where the extrapolation is not valid. In principle the particle could cross the grid in one large time step, then be bumped across the edge in the next step. In practice, particles were moved about 0.2 grids each time step. An estimate of the time step size can be made by solving for T in the quadratic equation,

$$\mathbf{r}(T) = \mathbf{r}(0) + \mathbf{v}(0)T + q/2m\ \mathbf{E}(\mathbf{r}(0))T^2,$$

where $\mathbf{r}(T)$ is evaluated to cross the radially symmetric grid in all six directions and the smallest positive T is actually used. Particles which pass through the r = 0 line are reflected by changing the sign of the radial component of the velocity.

The potential field around the hole has cylindrical symmetry, so the angular coordinate becomes important only when visualizing the actual three dimensional trajectory. However, the angular velocity component plays a significant role. Angular effects were accounted for by calculating the motion in three dimensions, then rotating the coordinate system to find the new r, z, v_r, v_z, v_θ. This technique was tested by tracking a particle with no electric field present and ensuring that it followed a straight line.

Implementation of model

An objective of this effort was to produce a fast microcomputer model which could be used to investigate ion collection by pin holes. Figure 3 shows the flow of the program used.

Solving the potential field takes a significant amount of time, 10 minutes on an Intel 80387 to solve an 80 X 160 grid, but this need only be done once. The time can be minimized by using as limited a computational grid as possible. Solution of the particle trajectories is fast due to the semi-analytical approach taken. Typically times steps were scaled to cross 0.2ths of a grid region.

The approximation for $\mathbf{r}$ used above to enable integration of the acceleration begins to break down when $(\mathbf{r}(t)-\mathbf{r}(0)) \bullet \nabla \mathbf{E}$ is not small compared to $\mathbf{E}(\mathbf{r}(0))$, as is the case near the hole edge. However when this occurs the particle is almost certainly collected, though the calculated trajectory and impact point may not be accurate. A calculation space with a radial dimension twenty times the hole size gives sufficiently accurate results.

Velocity Distribution

The effect of a Maxwellian velocity distribution can be addressed by adding incremental velocities to the incident velocity representative of the three dimensional velocity distribution. The results for each velocity element are weighted by the probability of a particle having an incident velocity near the tested velocity.

To calculate a focus factor for a given temperature, the three dimensional particle velocity space was broken into a grid. Division of the velocity space into approximately 3000 (18x18x9) elements yielded a reasonable simulation. Only half the Θ velocity is needed due to the symmetry of the problem. Each grid element was assigned a velocity vector representative of its position and a weight of the fraction of particles contained in it. Focus factors for each velocity grid element were then obtained. The net focus factor is then the sum of the focus factor/weight product.

DISCUSSION

Focus Factor

For particles whose initial velocity is normal to the surface, the focus factor is easy to find. All particles emitted from the upper boundary inside a certain radius, r_c, will be collected. The focus factor, that is the enhancement in total current collected is the ratio of the collecting area to the hole area, or $(r_c/r_h)^2$.

It is interesting that the impact points do not map monotonically with the incident radius. As shown in figure 4, both for particles near the center and far from the edge the further away from the center a particle is dropped, the further away it hits. But particles which traverse near the edge can end up almost anywhere.

The following dependencies were investigated for a base set of conditions simulating RAM impact conditions for SSF orbits, i.e.: oxygen ions, at normal incidence, with an initial velocity corresponding to 4.5 eV, and with a temperature of 0.1 eV.

Energy Dependence

A qualitative argument can be made to describe the focus factor's dependence on incident energy. In this model both the upper boundary (plasma sheath edge) and the lower boundary (surface) have the same potential. Therefore if the incident particle picks up more kinetic energy, due to motion directed parallel to the surface, than its initial incident energy, it will not be able to reach the lower surface except in the hole. If a particle is dropped into the grid with zero velocity and

temperature, except at the outside edge, it will reach the hole and the focus factor is essentially infinite.

In low earth orbit the focus factors will be smaller than those which are observed in ground tests since the ram energy of the incident ions is larger than the thermal energy of ions used in most ground tests.

Results of the calculated focus factor as a function of incident velocity are shown in figure 5.

Hole Size and the Plasma Sheath

The calculations presented here scale with two geometric parameters, the hole size relative to both the width and height of the calculation space. To obtain meaningful results the hole size should be small compared to the total surface area. Therefore the calculation grid should be wide enough that further expansion of the grid does not affect the trajectories of those particles which hit or nearly hit the hole.

On the other hand, the height of the calculation space indicates a distance above which the electric field is zero. Therefore it performs a function similar to the plasma sheath. These results obtained by changing the pinhole radius as compared to the sheath thickness are displayed in figure 6.

It is expected that as the hole size becomes large compared to the sheath the focus factor will approach unity. But in this case the height of the calculation space would be identified as the Child-Langmuir length. As the hole gets small compared to the height of the calculation space the focus factor will approach a value which depends only on incident angle and temperature, and incident energy. However, in these simulations, as the hole gets even smaller the focus factor drops off again. Possibly the particles cannot reach the hole due to angular momentum constraints.

Temperature

As indicated above, modeling temperature effects requires finding focus factors for a large number of initial velocities. Particles with high angles of incidence may hit the hole from considerable distances away. Fortunately these represent a small portion of the velocity space. The effect of temperature is shown in Figure 7 for two cases. Figure 7a shows a case where the temperature is small compared to the incident velocity. Figure 7b shows a case with zero incident velocity.

Comparison to Experiment

Vaughn (ref. 6) has measured ion currents to a hole. He measured the current to a 0.54 cm diameter hole biased at -140 V. The Argon plasma he used had a number density of 2×10^{12} m^{-3}, an electron temperature of 1.2 eV and an ion energy of 2.0 eV. An ion current of 0.5 μA was measured. This suggests a focus factor of 78, if an ion thermal current is used, to 22, if the ions are assumed to be flowing. Since there was a 2 V drop from the plasma source to the tank plasma, we assume the latter number is the correct value.

The sheath thickness for comparison was estimated by finding where $\partial E_b/\partial h$, from an average potential seen as a function of height, is equal to ϱ/ε_o from the plasma density. A sheath thickness of .018 m was estimated for the ram case, and .021 m for the thermal case. This model predicts a focus factor of 18 for the ram velocity case, and 8.5 for the thermal case. The agreement is good.

Katz et al (ref.7) have noted that an accurate model must include a good model of the sheath edge, and also must model the surface potentials near the hole accurately. They have noted that the surface near the hole is shielded from thermal electrons by the hole's negative potential and tends to charge positive.

CONCLUSION

The simple pinhole ion collection model presented here permits reasonable estimates of focus factors. The model uses a solution to Laplace's equation of the cylindrically symmetric potential field to evaluate electric fields near the hole, then tracks particles to evaluate the focus factor. The particles are tracked in three dimensions, though the angular coordinate can be ignored. The model permits incident velocities in three dimensions and can therefore be used to model temperature effects.

An objective of this work was to provide a fast model pin hole collection. Focus factors for specific initial velocities are found quickly but temperature calculations are time consuming due to the large number of particles tracked.

The present model assumes a level plasma sheath and a uniform surface potential. The accuracy of the model might be improved by including an analytical model of the sheath shape and the surface potential. We intend to verify the accuracy of the model further by comparing its result with I-V curves obtained in the ion collection tests.

ACKNOWLEDGMENTS

Parts of this work were sponsored by the NASA Lewis Research Center under contract NAS3-25266 with Dale C. Ferguson as monitor. The authors would like to thank Russell Cottam for valuable discussion and Thomas L. Morton for computer graphics.

REFERENCES

1. Stevens, N.J., Berkopec, F.D., Purvis, C.K., Grier, N., and Staskus, J., "Investigation of high voltage spacecraft interactions with plasma environments," AIAA/DGLR 13th International Electric Propulsion Conference Paper 78-672 (1978).

2. Gabriel, S.B., Garner, C.E. and Kitamura, S., "Experimental Measurements of the Plasma Sheath Around Pinhole Defects in a Simulated High-Voltage Solar Array," AIAA Paper 83-0311 (1983).

3. Chaky, R.C., Nonnast, J.H., and Enoch,J. "Numerical simulation of sheath structure and current-voltage characteristics of a conductor-dielectric in a plasma," J. Appl. Phys. 52(12), pp. 7092-7098 (1981).

4. Brandon, S.T., Rusk, R.L., Armstrong, T.P., and Enoch, J., "Self-Consistent Simulation of Plasma Interactions with Secondary-Emitting Insulators," Spacecraft Environmental Interactions Technology 1983, NASA CP 2359, pp 287-303 (1985).

5. Mandell, M.J., and Katz, I., "Surface Interactions and High-Voltage Current Collection," Spacecraft Environmental Interactions Technology 1983, NASA CP 2359, pp 305-319 (1985).

6. Vaughn, J., "Ion Focusing Test", Electrical Grounding Tiger Team Meeting, Huntsville, Al, May 14-17, 1991.

7. Katz, I., Davis, V.A., and Mandell, M.J., "Ion Focussing and Implications for SiO2 Deposition in Solar Array Gaps," Electrical Grounding Tiger Team Meeting, Huntsville, Al, May 14-17, 1991.

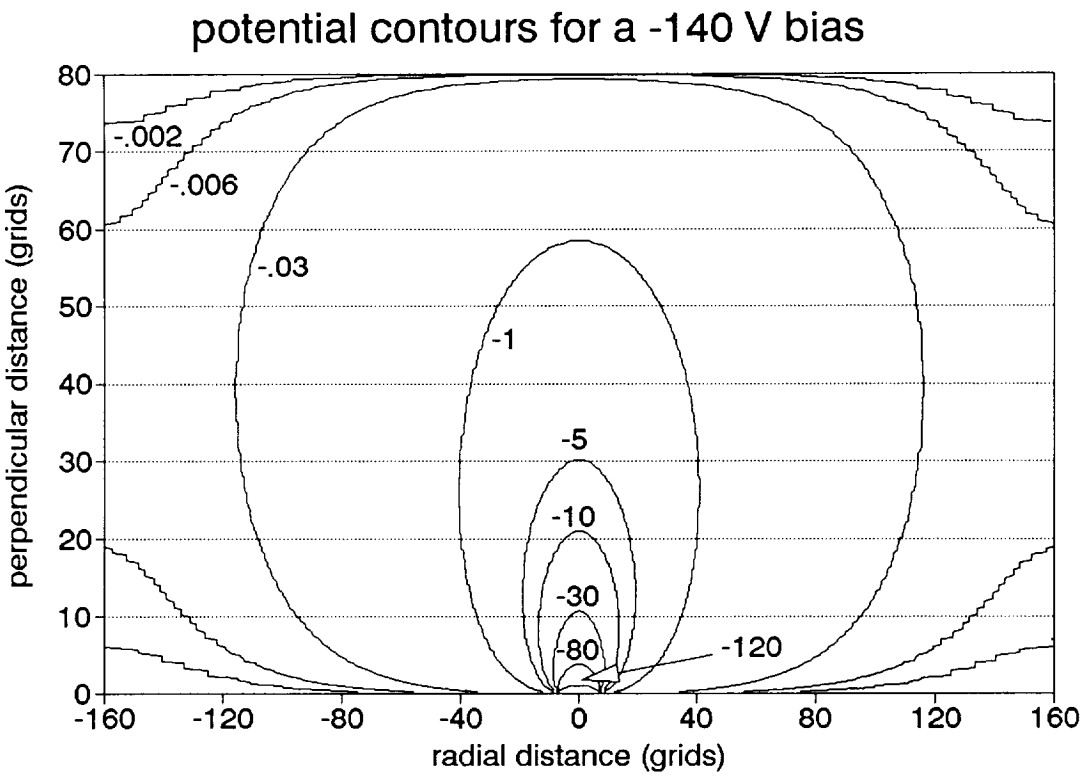

Figure 1. Potential contours near hole. Hole bias is -140 V and hole radius is 8 grids.

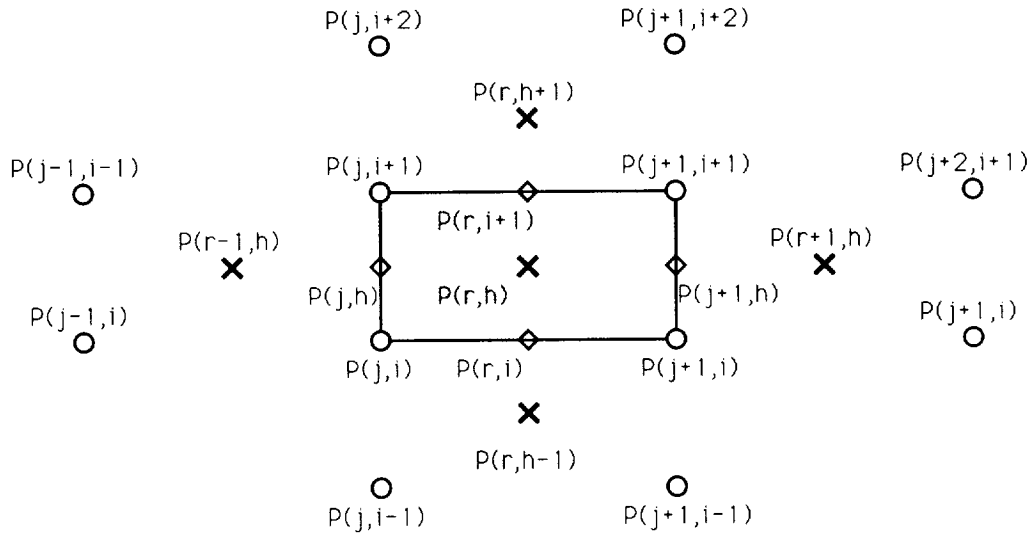

Figure 2. Potential interpolation scheme.

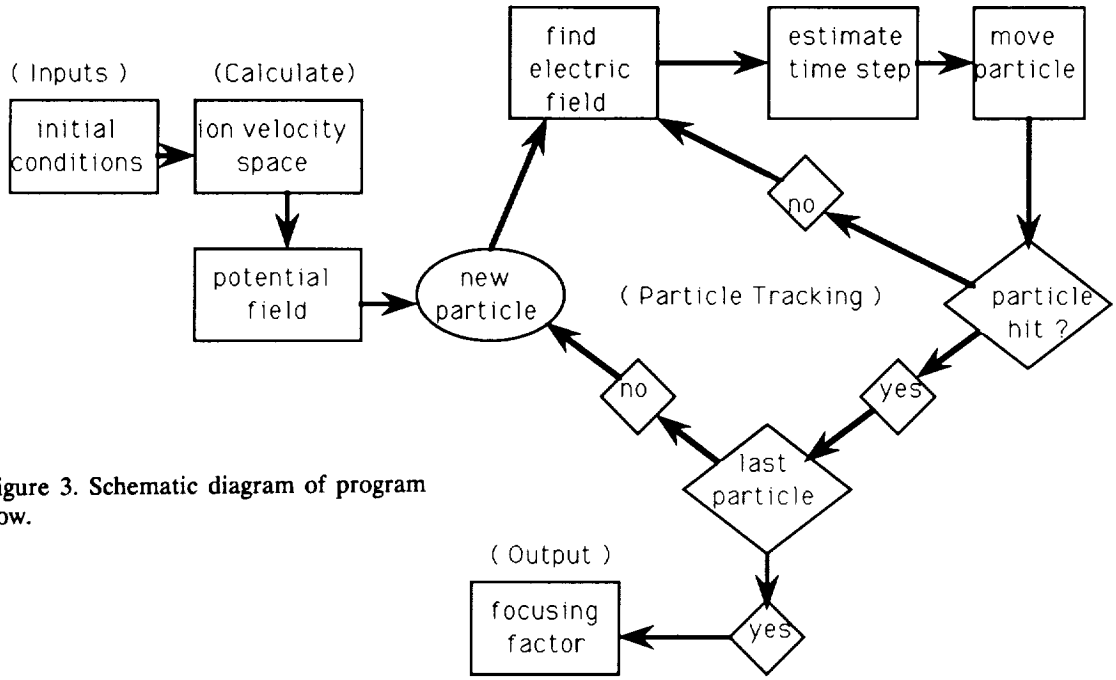

Figure 3. Schematic diagram of program flow.

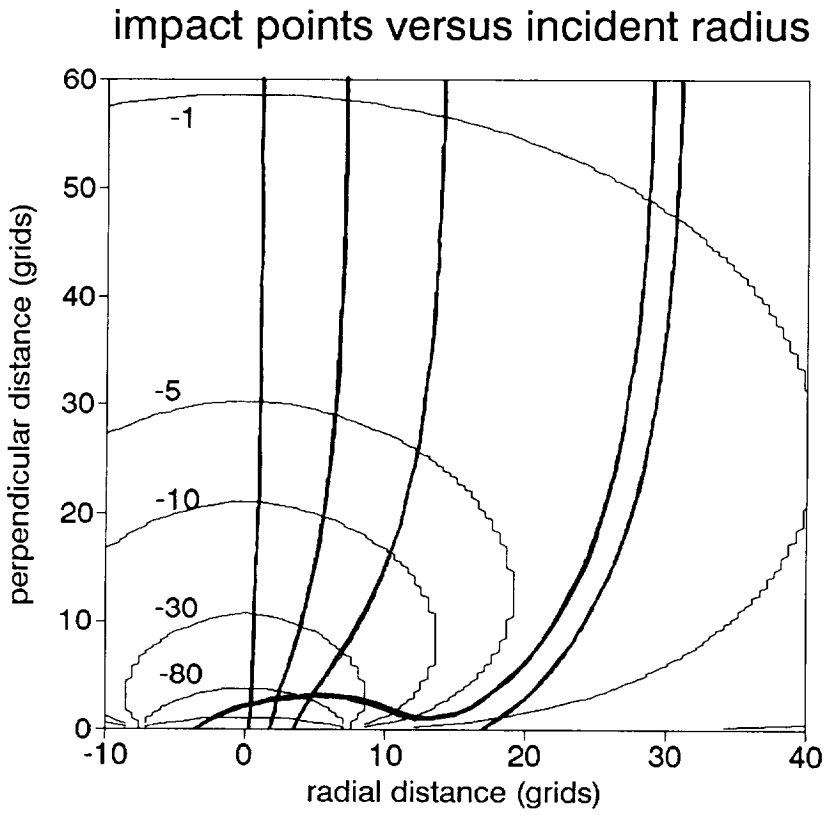

Figure 4. Examples of particle trajectories.

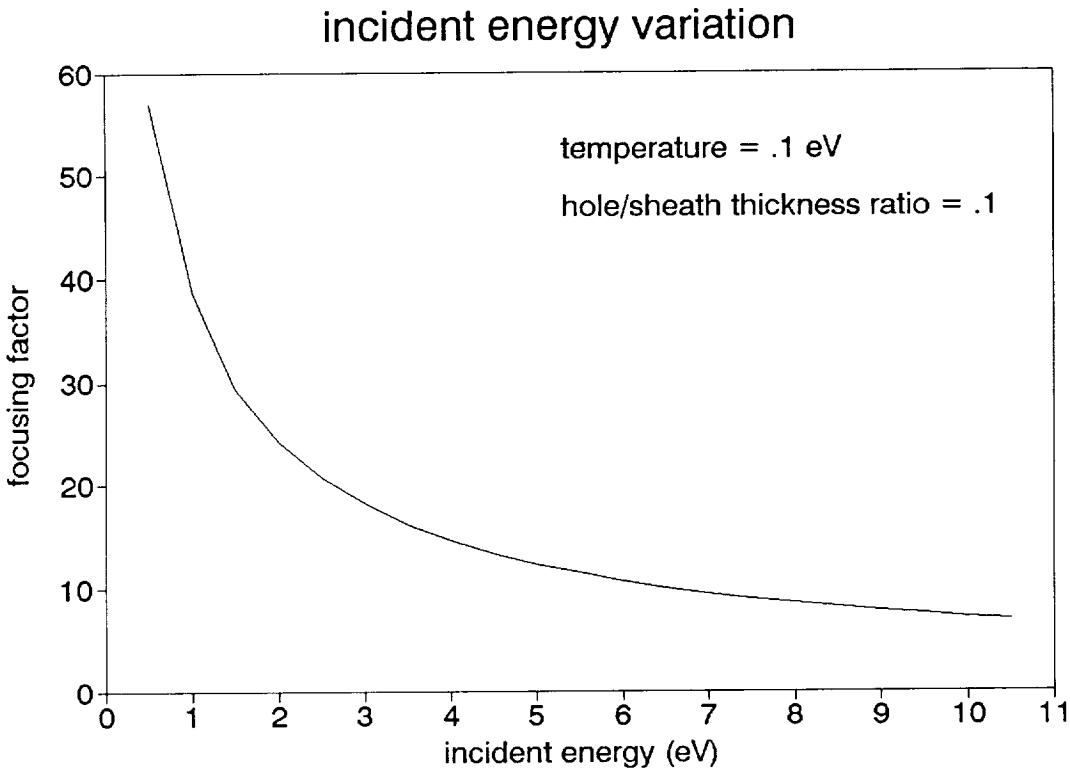

Figure 5. Relationship between energy of incident particles and resulting focus factor.

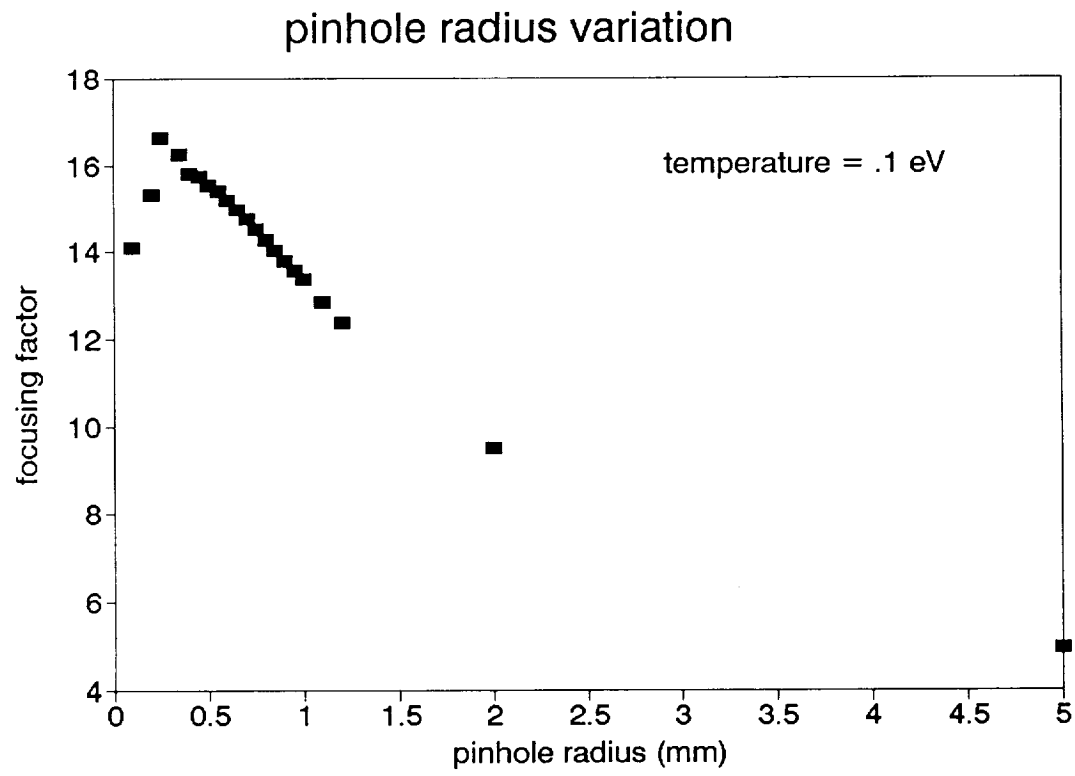

Figure 6. Effect of pinhole size on focus factor.

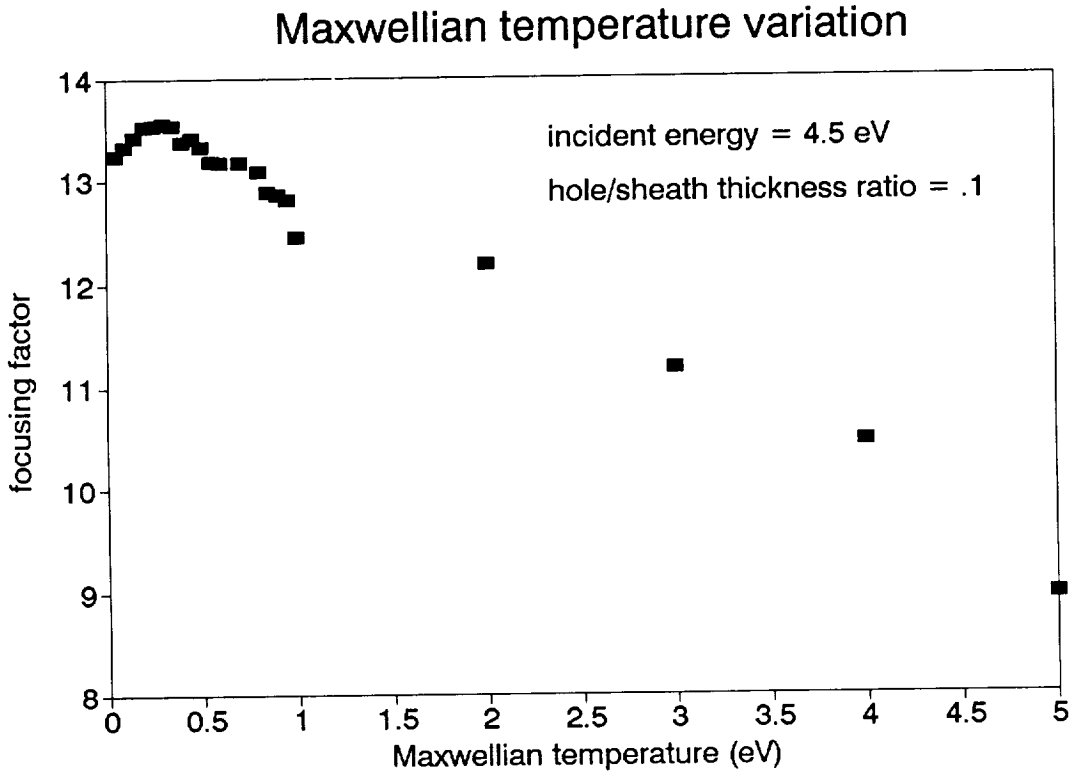

Figure 7a. Effect of temperature on focus factor.

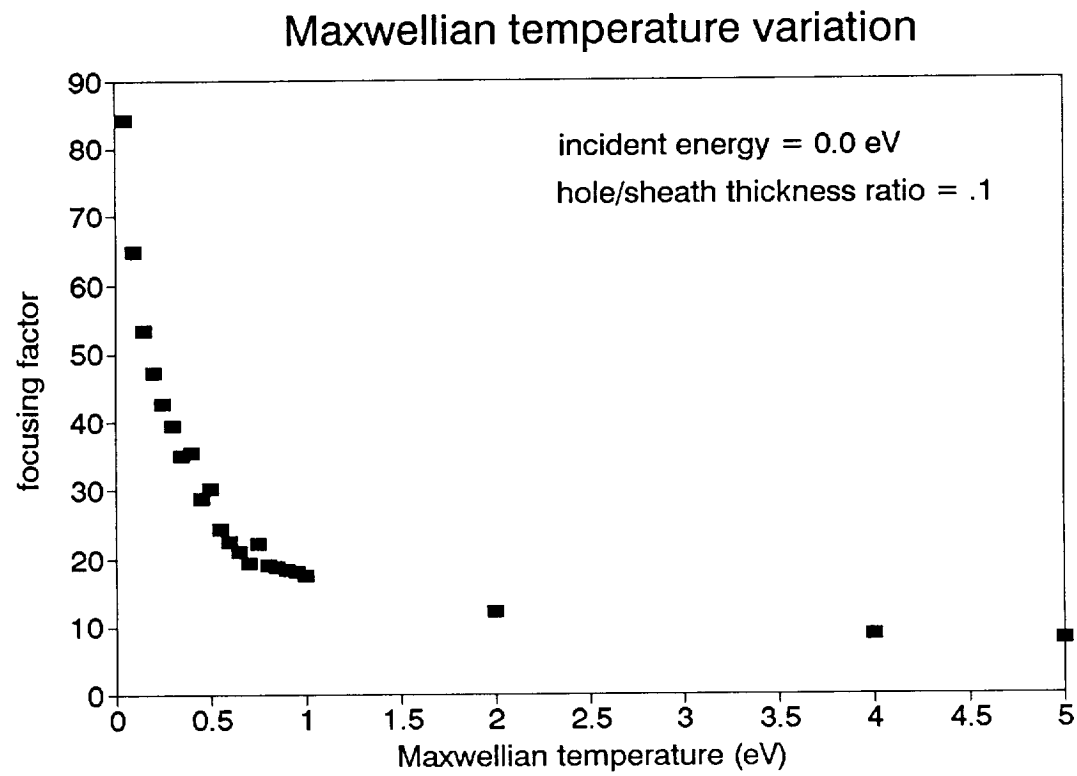

Figure 7b. Effect of temperature on focus factor.